

**Trench-parallel anisotropy produced by serpentine deformation in the
hydrated mantle wedge**

Ikuo Katayama¹, Ken-ichi Hirauchi¹, Katsuyoshi Michibayahi², Jun-ichi Ando¹

*¹Department of Earth and Planetary Systems Science, Hiroshima University,
Higashi-Hiroshima 739-8526, Japan*

²Institute of Geosciences, Shizuoka University, Shizuoka 422-8529, Japan

Corresponding author: Ikuo Katayama

Tel: +81-824-24-7468, Fax: +81-824-24-0735

E-mail: katayama@hiroshima-u.ac.jp

Seismic anisotropy is a powerful tool for detecting the geometry and style of deformation in the Earth's interior, as it primarily reflects the deformation-induced preferred orientation of anisotropic crystals^{1,2}. Although seismic anisotropy in the upper mantle is generally attributed to the crystal-preferred orientation of olivine³, the strong trench-parallel anisotropy ($\delta t \sim 1-2$ sec) observed in several subduction systems^{4,5} cannot be explained in terms of olivine anisotropy, even if the entire mantle wedge were to act as an anisotropic source. Here we show that the crystal-preferred orientation of serpentine, major hydrous mineral in the upper mantle, can produce the strong trench-parallel seismic anisotropy in subduction systems. High-pressure deformation experiments reveal that the pole of serpentine basal plane (*c*-plane) tends to rotate normal to the shear plane during deformation; consequently, seismic velocity propagating normal to the shear plane (plate interface) is much slower than that in other directions. The estimated seismic anisotropy for deformed serpentine aggregates ($\sim 32\%$ AVs) is an order of magnitude greater than that for olivine⁶; thereby the alignment of serpentine in the hydrated mantle wedge results in a strong

trench-parallel seismic anisotropy in the case of a steeply subducting slab. This hypothesis is consistent with the presence of a hydrous phase in the mantle wedge, as inferred from anomalously low seismic-wave velocities⁷.

The geometry and strength of seismic anisotropy are generally estimated by measuring shear-wave splitting, which constrains of the polarization direction of the fast shear-wave propagation and the delay time between the arrivals of the fast and slow shear waves. Measurements of shear-wave splitting above the mantle wedge in most subduction zones, including the Japan subduction system, reveal trench-parallel anisotropy⁸, in which the propagation direction of the fast shear-wave is oriented subparallel to the trench; however the delay time (δt) shows marked spatial variations (Fig. 1a). For example, δt is ~ 0.1 - 0.2 seconds in northeast Japan⁹, ~ 1 - 2 seconds in the Ryukyu arc⁴. Note that we focus on splitting data collected from local slab earthquakes as these provide direct constraints on seismic anisotropy of the mantle wedge.

The length of the delay time depends on the strength of the anisotropy and thickness of the anisotropic layer. If we consider that seismic anisotropy is caused by the

crystal-preferred orientation of olivine, the short delay time recorded in northeast Japan could be explained in terms of a relatively thin anisotropic layer in the mantle wedge¹⁰, whereas the longer delay time observed in the Ryukyu arc could not be explained in terms of olivine anisotropy, as the inferred anisotropic layer (~100-200 km) becomes thicker than the entire mantle wedge sampled by the local shear wave (Fig. 1b).

Serpentine has a strong crystallographic anisotropy (*AVs* of ~82% for lizardite single-crystal¹¹), approximately five times stronger than that for olivine (*AVs* of ~18%)¹², and the occurrence of serpentine is expected where water infiltrates into the mantle¹³. Accordingly, one possible explanation of the strong anisotropy observed in the Ryukyu arc is the crystal-preferred orientation of serpentine¹⁴. To test this hypothesis, we performed deformation experiments on serpentine under conditions corresponding to the mantle wedge, and analyzed the resulting deformation-induced crystallographic preferred orientation of serpentine in terms of its ability to explain the strong trench-parallel seismic anisotropy.

Deformation experiments were carried out at $P = 1$ GPa and $T = 300$ - 400°C at constant strain rate using a solid-medium apparatus (detailed in Supplementary

Information). The starting material of natural antigorite (a high-temperature form of serpentine), which exhibited near-isotropic texture, was sandwiched between alumina pistons cut at 45° from the maximum compression direction, oriented to represent the deformation geometry of simple shear. We made tiny grooves at the interface between the sample and piston to prevent slip during deformation. These materials were surrounded by a nickel jacket, and the oxygen fugacity was buffered by the Ni/NiO reaction. After pressure and temperature had reached the desired value, a piston was advanced at a constant rate. Shear strain was measured from the rotation of a nickel strain-marker that was initially orientated perpendicular to the shear direction.

The serpentine samples were deformed up to strains of $\gamma \sim 2.0$ in a dominantly simple-shear geometry (compressional strain was generally less than 10% of shear strain). The serpentine grains and trail of magnetite become significantly elongated, with the stretching axes oriented subparallel to the strain-marker (Fig. 2). The deformed serpentine showed undulatory extinction, suggesting intracrystalline deformation accommodated by the dislocation creep, which is consistent with the mechanical creep tests of serpentine¹⁵.

Figure 3 shows the crystallographic orientations of the deformed serpentine grains, as measured using electron backscatter diffraction (EBSD) technique at the Centre for Instrumental Analysis, Shizuoka University, Japan. Although the starting materials showed only a weak crystal-preferred orientation at most (Fig. 3a), the deformed serpentines in all experiments are characterized by a strong concentration of [001] axes normal to the shear plane and a relatively weak concentration of [100] axes subparallel to the shear direction (Fig. 3b,c). At higher strains, serpentine [100] axes are oriented close to the shear direction, whereas at lower strains the [100] maxima are tilted toward the finite strain ellipse (Fig. 3b). The strong alignment of serpentine (001) planes parallel to the shear plane is consistent with the pattern found in naturally deformed serpentinites¹⁶.

The serpentine fabric produced by the deformation experiments corresponds to seismic anisotropy characterized by a slow propagation direction oriented normal to the shear plane, as the layered crystallographic structure within serpentine (antigorite) results in a significantly slower seismic velocity propagating perpendicular to the basal (001) plane. Although a lack of elastic constants for antigorite due to the complexity of

crystal structure, we computed seismic anisotropy corresponding to the serpentine aggregates using elastic constants for lizardite serpentine¹¹ as a first approximation, which crystal structures and elastic properties are similar. The results show a strong seismic anisotropy for the deformed serpentine aggregates, up to 46% of P-wave azimuthal anisotropy and up to 32% of S-wave anisotropy at the highly strained sample of $\gamma \sim 2.0$ (Fig. 3e). These estimates nearly agree with the elastic wave measurements of naturally deformed serpentinites that reveal a strong anisotropy in the direction normal to foliation by up to AVs of $\sim 40\%$ ^{16,17}. Kern *et al.*¹⁶ demonstrated that the magnitude of anisotropy in serpentinite is relatively insensitive to pressure and temperature in the range of $P < 600$ MPa and $T < 600^\circ\text{C}$, but it may decrease at higher pressures due to the efficient compressibility along the serpentine [001] axis.

We now apply the above results in explaining seismic anisotropy within a subduction zone setting. In the Ryukyu arc, where the relatively young Philippine Sea Plate is subducting beneath the Eurasia Plate at a steep angle ($\sim 45^\circ$)¹⁸, water is released by dehydration reactions that occur in the subducting crustal materials, leading to the formation of serpentine (the main hydrous mineral in the upper mantle) in the overlying

mantle wedge. Deformation is primarily induced by the movement of the subducting plate with a dextral sense of shear, and shear strain is mainly accommodated in the regions above the plate interface. In such regions, the serpentine aggregates have the [100] axis in the down-dip slab direction parallel to the shear direction and the pole of (001) plane normal to the shear plane, and the [010] axis parallel to the trench axis (Fig. 4). Consequently, the shear wave that is polarized normal to the trench becomes significantly slower than the trench-parallel direction, resulting in a polarization of the fast shear wave parallel to the trench axis (trench-parallel anisotropy). The magnitude of detectable shear-wave splitting in the horizontal plane can be approximately half of the maximum shear-wave anisotropy generated across the serpentine basal plane and the other direction owing to the slowest [001] axis tilting 45 degree from the horizontal plane. This figure represents a minimum estimate of the seismic anisotropy as the serpentine [001] axis may be slightly tilted toward the continent side of the shear zone, and a greater contribution of the [001] axis within the horizontal plane results in a slower seismic velocity oriented normal to the trench. Moreover, natural strain can be much larger than that in laboratory experiments, suggesting that the strength of

anisotropy might be greater in the natural system.

Based on the above results, we conclude that alignment of serpentine in the mantle wedge results in a strong trench-parallel anisotropy ($AVs \sim 32\%$), whereas olivine crystal-preferred orientation produces a much weaker anisotropy ($AVs \sim 2-4\%$)⁶, resulting in turn in the shear-wave splitting with a relatively short delay time. The strong trench-parallel anisotropy observed in other subduction systems, including the Tonga-Kermadec arc⁵, may also result from the serpentine crystal-preferred orientation in association with a steeply dipping slab.

Several models have been proposed to explain the origin of trench-parallel anisotropy in subduction zones, including slab rollback¹⁹, 3D corner flow²⁰, convection driven by crustal delamination²¹, and deformation under water-rich condition²²; however, in these previous models, seismic anisotropy is mainly attributed to the crystal-preferred orientation of olivine. In contrast, we proposed that strong trench-parallel anisotropy of $\delta t \sim 1-2$ sec can result from the crystal-preferred orientation of serpentine in the hydrated mantle wedge. Even if trench-parallel flow is dominant in the forearc mantle^{5,20}, the basal plane of serpentine becomes aligned subparallel to the flow direction, thereby

producing a strong trench-parallel anisotropy. On the one hand, for mantle corner flow with a shallow dipping angle, seismic anisotropy becomes weak as a result of less contribution of the [001] axis on the horizontal plane. Trench-parallel anisotropy has recently been ascribed to the occurrence of serpentine-filled faults in the subducting slab²³. We cannot preclude this hypothesis because of the poor vertical resolution in the measurements of seismic anisotropy⁸; however, our model predicts that the anisotropy is mainly generated by flow in the mantle wedge, consistent with measurements of local S-waves sampled mostly through the mantle wedge⁴.

The spatially variable nature of trench-parallel anisotropy in northeast Japan ($\delta t \sim 0.1-0.2$ sec)⁹ and the Ryukyu arc ($\delta t \sim 1-2$ sec)⁴ may reflect the heterogeneous distribution of serpentine. Serpentinization of the mantle wedge is primarily controlled by the subduction geotherm²⁴; in a relatively warm subduction zone, such as the Ryukyu arc, large amounts of water are released at shallow depths (~ 40 km) via dehydration reactions that occur in the subducting plate, migrating into the overlying mantle and causing extensive serpentinization; in contrast, most dehydrations are limited at deeper levels (>100 km) in cool subduction zones and serpentinization is not expected in the

shallow parts of the mantle wedge, such as that in northeast Japan.

Seismic tomography reveals an extensive low-velocity anomaly in the mantle wedge beneath Ryukyu⁷, suggesting the occurrence of serpentine, whereas such an anomaly is rarely observed in the forearc mantle beneath northeast Japan²⁵. Our model does not resolve the anisotropic source of shear-wave splitting with a short delay time, but our results indicate that a strong trench-parallel anisotropy ($\delta t \sim 1-2$ sec) can be produced by the crystal-preferred orientation of serpentine in a hydrated mantle wedge.

References

1. Nicolas, A. & Christensen, N. I. in *Composition, Structure and Dynamics of the Lithosphere-Asthenosphere System* (eds Fuchs, K. & Froideveaux, C.) 407-433 (American Geophysical Union, Washington, DC, 1987).
2. Long, M. D. & Silver, P. G. The subduction zone flow field from seismic anisotropy: A global view. *Science* **319**, 315-318 (2008).
3. Zhang, S. & Karato, S. Lattice preferred orientation of olivine aggregates deformed in simple shear. *Nature* **375**, 774-777 (1995).

4. Long, M. D. & van der Hilst, R. D. Shear wave splitting from local events beneath the Ryukyu arc: Trench-parallel anisotropy in the mantle wedge. *Phys. Earth Planet. Inter.* **155**, 300-312 (2006).
5. Smith, G. P., Wiens, D. A., Fisher, K. M., Dorman, L. M., Webb, S. C. & Hildebrand, J. A. A complex pattern of mantle flow in the Lau backarc. *Science* **292**, 713-716 (2001).
6. Katayama, I. & Karato, S. Effect of temperature on the B- to C-type olivine fabric transition and implication for flow pattern in subduction zones. *Phys. Earth Planet. Int.* **157**, 33-45 (2006).
7. Wang, Z., Huang, R., Huang, J. & He, Z. P-wave velocity and gradient images beneath the Okinawa trough. *Tectonophys.* **455**, 1-13 (2008).
8. Wiens, D.A., Conder, J. A. & Faul, U. H. The seismic structure and dynamics of the mantle wedge. *Annu. Rev. Earth Planet. Sci.* **36**, 421-455 (2008).
9. Nakajima, J. & Hasegawa, A. Shear-wave polarization anisotropy and subduction-induced flow in the mantle wedge of northeastern Japan. *Earth Planet. Sci. Lett.* **225**, 365-377 (2004).

10. Katayama, I. Thin anisotropic layer in the mantle wedge beneath northeast Japan. *Geology* **37**, 211-214 (2009).
11. Auzende, A. L., Pellenq, R. J. M., Devouard, B., Baronnet, A. & Grauby, O. Atomistic calculations of structural and elastic properties of serpentine minerals: the case of lizardite. *Phys. Chem. Minerals* **33**, 266-275 (2006).
12. Abramson, E. H., Brown, J. M., Slutsky, L. J. & Zaug, J. The elastic constants of San Carlos olivine to 17 GPa. *J. Geophys. Res.* **102**, 12253-12263 (1997).
13. Hyndman, R. D. & Peacock, S. M. Serpentinization of the forearc mantle. *Earth Planet. Sci. Lett.* **212**, 417-432 (2003).
14. Kneller, E. A., Long, M. D. & van Keken, P. E. Olivine fabric transitions and shear wave anisotropy in the Ryukyu subduction system. *Earth Planet. Sci. Lett.* **268**, 268-282 (2008).
15. Hilairet, N., Reynard, B., Wang, Y., Daniel, I., Merkel, S., Nishiyama, N. & Petitgirard, S. High-pressure creep of serpentine, interseismic deformation, and initiation of subduction. *Science* **318**, 1910-1913 (2007).
16. Kern, H., Liu, B. & Popp, T. Relation between anisotropy of P and S wave

- velocities and anisotropy of attenuation in serpentinite and amphibolite. *J. Geophys. Res.* **102**, 3051-3065 (1997).
17. Watanabe, T., Kasami, H. & Ohshima, S. Compressional and shear wave velocities of serpentinitized peridotites up to 200 MPa. *Earth Planets Space* **59**, 233-244 (2007).
18. Li, C., van der Hilst, R. D. & Toksoz, M. N. Constraining P-wave velocity variations in the upper mantle beneath Southeast Asia. *Phys. Earth Planet. Int.* **154**, 180-195 (2006).
19. Buttles, J. & Olson, P. A. A laboratory model of subduction zone anisotropy. *Earth Planet. Sci. Lett.* **164**, 245-262 (1998).
20. Kneller, E. A. & van Keken, P. Trench-parallel flow and seismic anisotropy in the Mariana and Andean subduction systems. *Nature* **450**, 1222-1225 (2007).
21. Behn, M. D., Hirth, G. & Kelemen, P. Trench-parallel anisotropy produced by foundering of arc lower crust. *Science* **317**, 108-111 (2007).
22. Jung, H. & Karato, S. Water-induced fabric transitions in olivine. *Science* **293**, 1460-1463 (2001).
23. Faccenda, M., Burlini, L., Gerya, T. & Mainprice, D. Fault-induced seismic

- anisotropy by hydration in subducting oceanic plates. *Nature* **455**, 1097-1101 (2008).
24. Hacker, B. R., Abers, G. A. & Peacock, S. M. Subduction factory 1. Theoretical mineralogy, densities, seismic wave speeds, and H₂O contents. *J. Geophys. Res.* **108**, doi:10.1029/2001JB001127 (2003).
25. Nakajima, J., Matsuzawa, T., Hasegawa, A. & Zhao, D. Three-dimensional structure of V_p, V_s and V_p/V_s beneath northeast Japan: Implications for arc magmatism and fluids. *J. Geophys. Res.* **106**, 21843-21857 (2001).
26. Nakajima, J., Shimizu, J., Hori, S. & Hasegawa, A. Shear-wave splitting beneath the southwestern Kurile arc and northeastern Japan arc. *Geophys. Res. Lett.* **33**, L05305 (2006).

Acknowledgements

We thank T. Watanabe and S. Karato for comments and discussions. D. Mainprice and A. Tommasi are appreciated for providing the crystallographic files of serpentine. This study was supported by the Japan Society for the Promotion of Science (JSPS).

Figure captions

Fig. 1. Observations of shear-wave splitting in the Japan subduction system. a,

Shear-wave splitting from local S-phases along the Ryukyu arc⁴ and northeast Japan^{9,26}.

The orientations of bars correspond to the fast polarization direction, and the bar lengths

are normalized to the average delay time. **b,** Relation between shear-wave delay time

and thickness of anisotropic layer assuming olivine and serpentine as a source. If we

employ the strength of anisotropy based on experimentally deformed B-type olivine

aggregates (*AVs* of 4.5%)⁶ or highly deformed serpentine in this study (*AVs* of 32%), the

longer delay time (1-2 s) observed in the Ryukyu arc require an anisotropic thickness of

100-200 km in the case for olivine, whereas 10-20 km thickness for serpentine.

Fig. 2. Optical microphotograph of deformed serpentine after experiments. a,

Viewed in plane-polarized light. **b,** Viewed with the gypsum plate inserted. The sample

is sandwiched between alumina pistons, and the thin dark layer is a nickel strain-marker,

which was originally oriented normal to the shear plane. Arrows indicate the sense of

shear. The sample consists mainly of antigorite, with minor magnetite (opaque grains).

The serpentine grains and trails of magnetites are significantly elongated subparallel to the strain-marker, and the highly strained grains show undulatory extinction (subgrains).

Fig. 3. Pole figures and seismic anisotropy of serpentine aggregates. **a**, Starting material. **b,d**, Sample deformed at $T = 400^{\circ}\text{C}$ and $\gamma = 0.8$. **c,e**, Sample deformed at $T = 300^{\circ}\text{C}$ and $\gamma = 2.0$. For the experimentally deformed samples, the east-west direction corresponds to the shear direction (sense of shear is dextral), and north-south is normal to the shear plane. Both runs are characterized by a strong concentration of [001] axes normal to the shear plane and a relatively weak concentration of [100] axes subparallel to the shear direction. The other two runs show similar patterns, but have slightly weaker fabrics. In the pole figure, equal-area lower-hemisphere projections were used with a Gaussian half-width angle of 8.5 degree, and the counters represent the density of data points (multiples of uniform density) of 150-200 grains for each sample. Seismic anisotropy was calculated using the elastic constants for lizardite¹¹. The pole figures and seismic anisotropy were prepared using the software written by D. Mainprice.

Fig. 4. Schematic diagram showing the cross section of the Ryukyu arc. Serpentine formed in the mantle wedge due to the infiltration of water expelled from the subducting plate, and deformation could be mostly accommodated in a relatively thin layer above subducting plate. In such regions, the seismically slowest axis in serpentine (*c*-axis) tends to align normal to the plate interface, resulting a strong trench-parallel anisotropy in the case of steeply subducting slab, such as the Ryukyu arc.

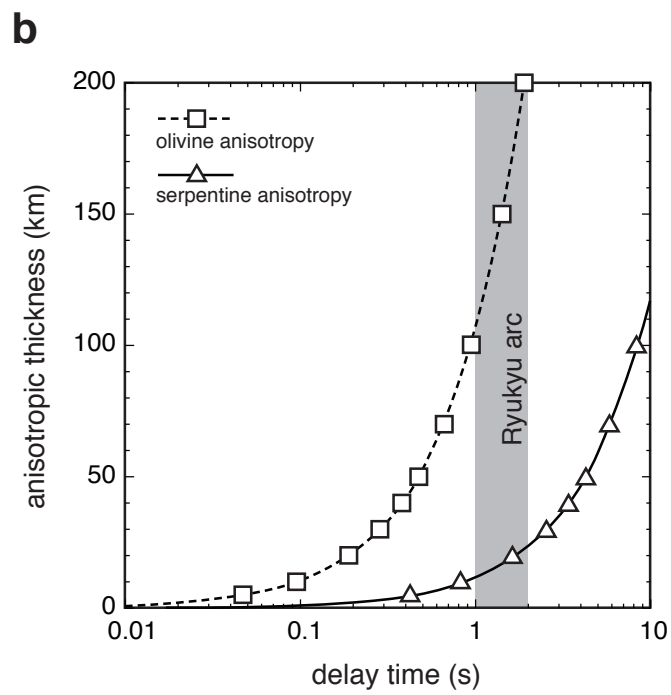
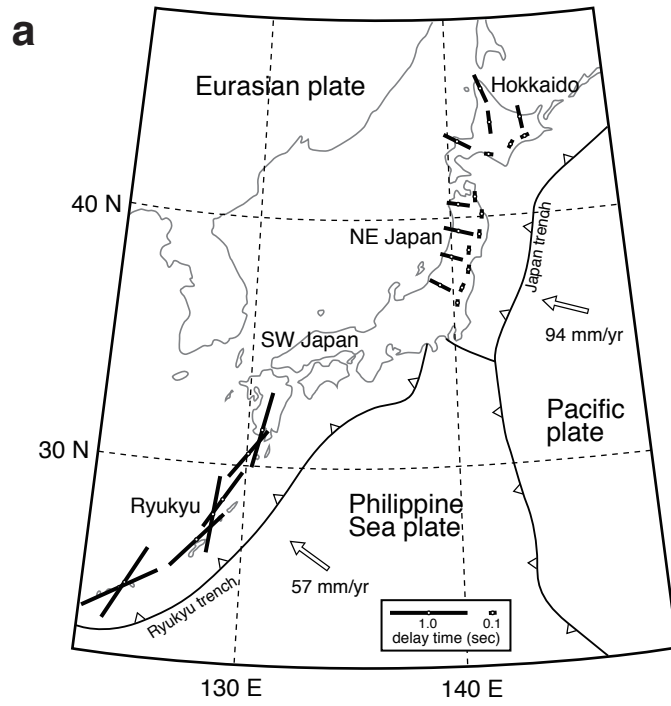


Fig. 1. Katayama et al.

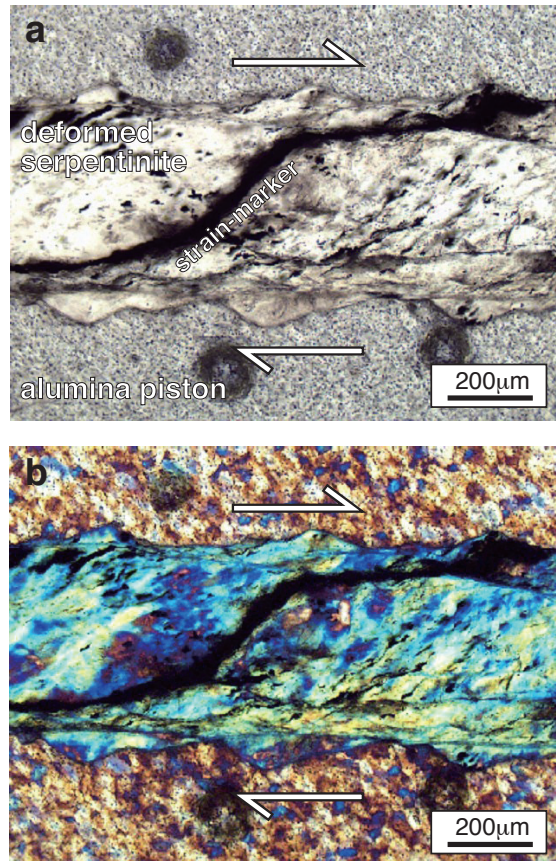


Fig. 2 Katayama et al.

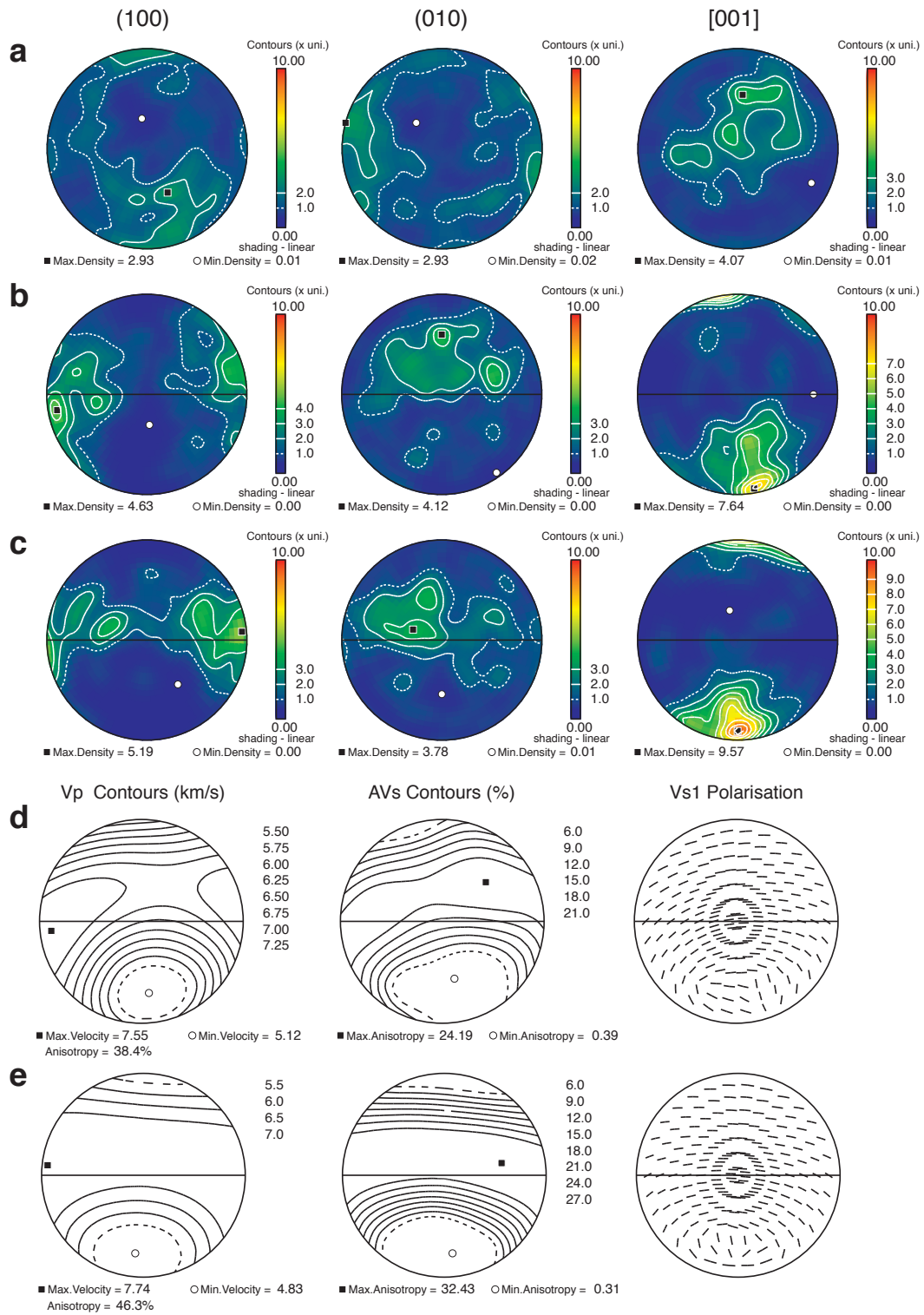


Fig. 3. Katayama et al.

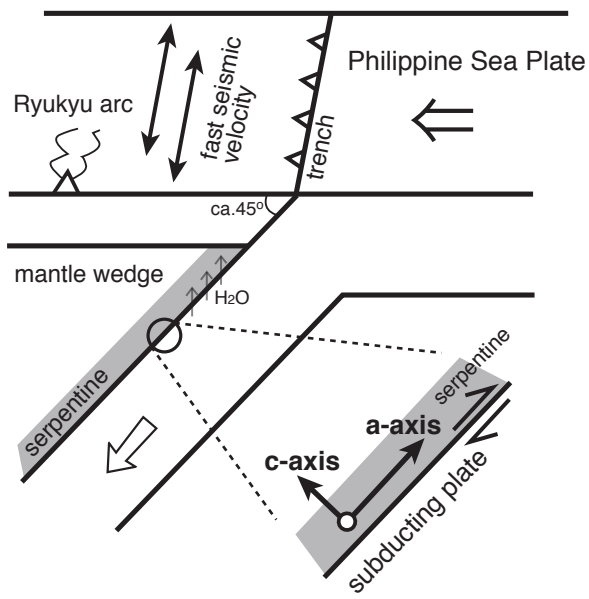


Fig. 4. Katayama et al.